

Structural, optical, and electrical properties of the $\text{Si}_{10}\text{Ge}_{10}\text{As}_x\text{Te}_{80-x}$ amorphous system

Ibrahim A. Saleh¹, Tarek M. Fayez²

¹Physics Department, Faculty of Arts and Science-Al Abyar, Benghazi University, Libya

²Physics Department, Faculty of Science, Sebha University, Libya

Article information	Abstract
<p>Key words</p> <p><i>Multilayers system, optical band gap, activation energies, electrical conductivity, photoluminescence.</i></p> <p>Received 22/06/ 2025, Accepted 08 / 07 / 2025, Available online 09 / 07 /2025</p>	<p>The thin films of the system $\text{Si}_{10}\text{Ge}_{10}\text{As}_x\text{Te}_{80-x}$ (where $x = 5$ and 15) prepared at 80°C were studied in the temperature ranges of 200, 300, and 400°C. The two multilayers of thin films consist of silicon (Si), germanium (Ge), and tellurium (Te) doped with arsenic (As). Annealing temperature was varied to investigate its effect on the structural and electrical properties of the films. The crystalline structure and the influence of annealing on the structure were investigated by X-ray diffraction. The X-ray data of films annealed at 400°C illustrated some crystallizing Ge-Ge phases. The optical band gap decreasing of arsenic-doped films was found. It has been shown that with increasing arsenic content in the films, their conductivity also increases. The optical measurements showed that the optical energy gap E_g decreases and/or increases upon annealing, while the increase is partially due to crystallization effects. Regarding the electrical measurements, they were carried out at different annealed temperatures and annealing times. The results showed that band gap energy decreases from 2.49 to 1.22 eV with respect to the rise of As content. Moreover, the incorporation of arsenic leads to a decrease in the activation energies of crystallization and an increase in the conductivity. The activation energies of crystallization of the As-(15nm) and As-(45nm)-doped systems $\text{Si}_{10}\text{Ge}_{10}\text{As}_x\text{Te}_{80-x}$ are 16.9 and 11.5 kJ/mol, respectively.</p>

I. Introduction

The non-crystalline state of IR-transmitting materials, such as chalcogenides, is the subject of deep investigations due to their importance in preparing optical memories and their optical applications [1,2]. The Si-Ge-As-Te system has special interest due to its phase-change transition. Various works have reported thermal, electrical, optical, and structural studies of Si-Ge-As-Te glasses [1,2,3,4,5,6]. Most of these works showed the reversible switching phenomenon. The phase-change memory material is an important field because of quicker response, longer life, better scaling ability, and lower power consumption. Si-Ge-As-Te glasses seem to govern the switching phenomena, namely an amorphous–amorphous transition. The preparation method for this material therefore plays an important role in the morphological characteristics and control over the particle size and surface area [7,8]. The science of this field has contributed to the progress of electronic and optical devices and their

systems, which has had significant impacts on high-level information society [9,10,11]. Nanostructured materials are expected to advance in thermal management, as they are increasingly used in electronic and optical devices, despite less advanced control of material properties [12]. Nowadays, quaternary materials have shown more advantages over ternary alloys due to the doping of appropriate elements. The annealing dependence of optical parameters of the investigated material could be used for phase change memory devices and optoelectronics applications [13]. In the present work, preparation and characterization for multilayers of Si₁₀Ge₁₀As_xTe_{80-x} thin films by simple and low-cost techniques have been reported and were deposited using an Edwards 306 thermal evaporator under a vacuum of 6×10^{-5} mbar on borosilicate glass substrates. The configuration consists of silicon (Si), germanium (Ge), and tellurium (Te) doped with arsenic (As). The films were characterized by X-ray diffraction (XRD), conductivity, and optical measurements; after that, the results are reported and discussed. The main motivation of this work is to enhance the structural, electrical, and optical properties of Si-Ge-based thin films by doping them with arsenic (As) and tellurium (Te). The study aims to investigate the effects of annealing temperature and arsenic concentration on the crystallization behavior, electrical conductivity, and optical band gap of the films.

II. Experimental

The materials doped semiconductors are expected to progress in this field, as they have for electronic and optical devices. The elements tellurium and arsenic have been added to amorphous elements such as Si and Ge to improve the different properties. Two configurations of multilayers for thin films of the system Si₁₀Ge₁₀As_xTe_{80-x} (where $x = 5$ and 15) prepared at 80°C were deposited using the Edwards 306 thermal evaporator under a vacuum of 6×10^{-5} mbar on borosilicate glass substrates. The process of measuring film thickness begins by determining the mass of the evaporated material inside the evaporation chamber. This determination is based on the equation $m = 4\pi\rho R^2t$ [14], where m is the mass of the evaporated material, ρ is the density of the film material, R is half the distance between the evaporation chamber and the substrate holder where the film deposition occurs, and t is the estimated film thickness. This equation determines the mass of the material placed in the evaporation chamber to obtain the desired thickness. The thickness of the sample is technically calculated by the quartz crystal thickness monitor during the evaporation process. The configuration consists of Si, Ge, and Te doped with As. The first sample in this configuration is Si₁₀Ge₁₀As₅Te₇₅ with 15 nm of As is deposited. The thicknesses of the layers of this sample are 30 nm of Si, 30 nm of Ge, and 225 nm of Te. The second sample is Si₁₀Ge₁₀As₁₅Te₆₅. In this sample, 45 nm of As is deposited, and the thickness of Te is reduced to 195 nm. The samples of the two configurations are then annealed under vacuum at an eutectic temperature of 400 °C to form alloys between the deposited layers. The two samples were measured by X-ray diffractometer and spectrophotometer for structure analysis and transmission and absorption, respectively. Moreover, a closed-cycle cryostat was used for electrical measurements. The sample is maintained between two electrodes as a coplanar structure attached to a DC voltage of 60 volts. The pressure is about 6×10^{-3} mbar, depending on the geometry of the vacuum chamber. The substrate holder is provided by a heating system to raise the temperature of the sample up to 600°C. The two samples were measured by the photoluminescence spectrometer to measure the recombination lifetime and the optical transitions of the prepared samples.

III. Results and discussion

a. The X-ray diffraction (XRD)

The structural properties of multilayers for thin films of the system $\text{Si}_{10}\text{Ge}_{10}\text{As}_x\text{Te}_{80-x}$ (where $x = 5$ and 15) prepared at 80°C and annealed at 400°C have been investigated by XRD as shown in figure (1). The phases that appeared in the X-ray spectra are Ge-Ge(111), Ge-Ge(200), and Ge-Ge(211). The interplaner distances (d-spacing) have been calculated using Bragg's equation and are given in table (1). It is clear from X-ray analysis of multilayers for the system that crystallization effects occur only in the Ge matrix because of the crystallizing temperature of Ge (about 300°C). It is lower than that of silicon, arsenic, and tellurium (the annealing temperature was about 400°C while the temperature of crystallization was higher than that). These results indicate that arsenic and tellurium atoms are located between crystalline multilayers, those atoms for doped bonds with the surrounding atoms.

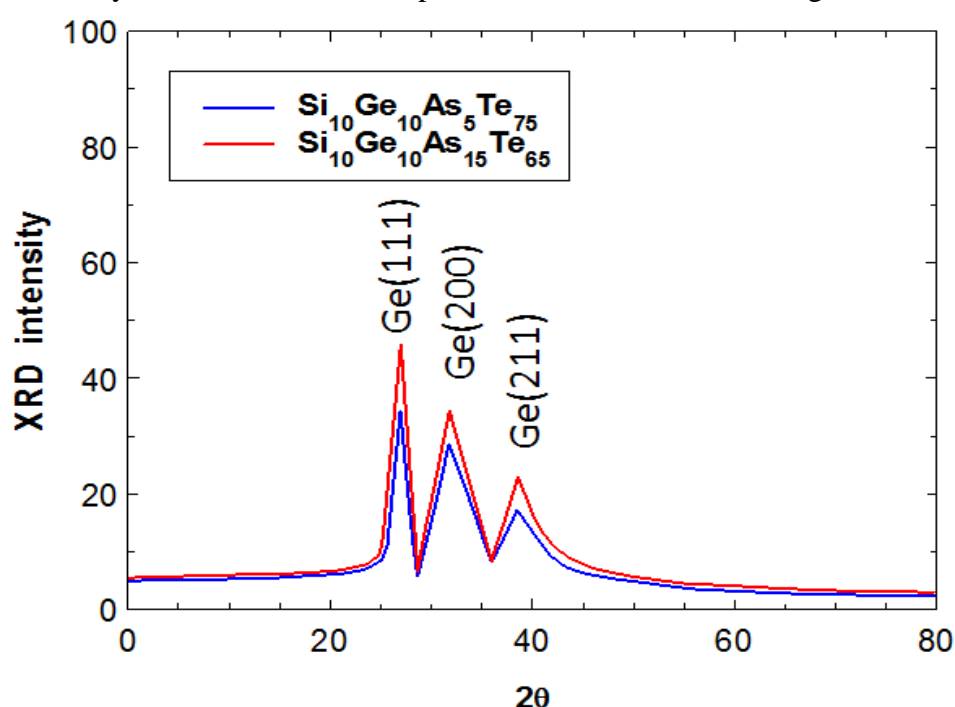


Figure (1): XRD spectra of multilayers for thin films of the system $\text{Si}_{10}\text{Ge}_{10}\text{As}_x\text{Te}_{80-x}$ (where $x = 5$ and 15) prepared at 80°C and annealed at 400°C for 2 h.

Table (1): The d-spacing of multilayers for thin films of the system $\text{Si}_{10}\text{Ge}_{10}\text{As}_x\text{Te}_{80-x}$ (where $x = 5$ and 15) prepared at 80°C after annealing at 400°C for 2 h.

Phases	(2θ) 2Theta	d-Spacing (Å)	$h^2+k^2+l^2$	Orientations	Lattice constant (Å)
Ge(111)	26.972	3.302	3	(111)	5.720
Ge(200)	31.717	2.818	4	(200)	5.636
Ge(211)	38.460	2.338	6	(211)	5.727

b. Optical properties

In this section, the optical energy gaps E_g and Urbach energy E_u after annealing at 400°C for 2h of the sample multilayers were determined. Figures (2) show the relation

between $(\alpha h\nu)^{1/2}$ and $(h\nu)$ for the samples according to Tauc's relation [15]: $(\alpha h\nu)^{1/2} = B(h\nu - E_g)$ where B is a constant and $h\nu$ is the photon energy. Figure (3) shows the relation between the inverse slope of $\log(\alpha(\omega))$ vs. $h\omega$ for the samples that according to the relation: $\alpha(\omega) = \alpha_0 \exp[h\omega/E_u]$, where the plot will give the Urbach parameter, E_u , to quantify the valence band tail characteristics [15,16,17]. The values of optical energy gap E_g and Urbach energy E_u deduced from the plots are given in table (2) for the two samples after annealing at 400°C for 2h. The data shows that the optical energy gap decreases while the Urbach energy increases mainly with raising and/or annealing temperature and due to the increasing doping of the arsenic (As-doped) with decreasing concentration tellurium (Te) and partially due to crystallization effects in Ge matrix. The incorporation of arsenic leads to a significant increase in carrier concentration, indicating that arsenic impurity atoms act as strong donor impurities. The self-compensation process is causing the (Si-Ge-Te:As) film to be in p-type form, despite arsenic acting as a co-activation donor [18].

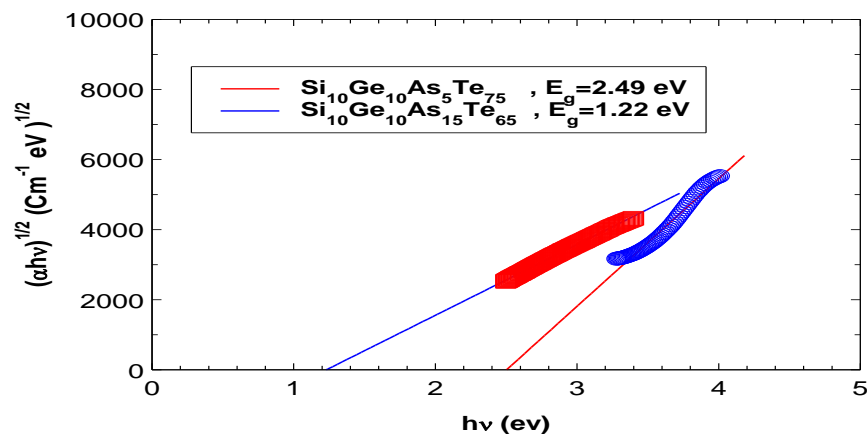


Figure (2): $(\alpha h\nu)^{1/2}$ vs. $(h\nu)$ for $\text{Si}_{10}\text{Ge}_{10}\text{As}_x\text{Te}_{80-x}$ (where $x = 5$ and 15) multilayers of (As-doped) after annealing at 400°C for 2 h.

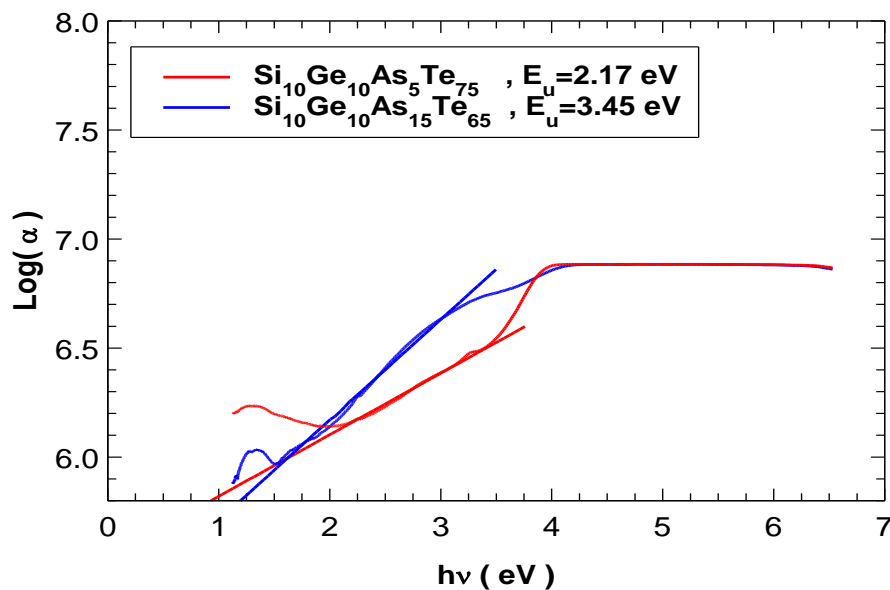


Figure (3): $\log(\alpha)$ vs. $h\nu$ for $\text{Si}_{10}\text{Ge}_{10}\text{As}_x\text{Te}_{80-x}$ (where $x = 5$ and 15) multilayers of (As-doped) after annealing at 400°C for 2 h.

Table (2): The optical band gap E_g and Urbach energy, E_u for untreated a-Si:H(3nm)/a-Ge:H multilayers of (As-doped).

Samples	(As-doped)	E_g (eV)	E_u (eV)
$\text{Si}_{10}\text{Ge}_{10}\text{As}_5\text{Te}_{75}$	15nm	2.49	2.17
$\text{Si}_{10}\text{Ge}_{10}\text{As}_{15}\text{Te}_{65}$	45nm	1.22	3.45

c. Electrical properties

i. The effect of material composition and annealing temperature on electrical conductivity

The electrical conductivity as a function of temperature for the As-doped system $\text{Si}_{10}\text{Ge}_{10}\text{As}_x\text{Te}_{80-x}$ (where $x = 5$ and 15) is amorphous in a range of different temperatures starting from 35°C ; the maximum temperature was 400°C , as shown in Figure (4). It is seen that the relation between the electrical conductivity and the temperature obeys the Arrhenius-type equation [19]: $\sigma = \sigma_0 e^{-E_a/k_B T}$ where σ is the electrical conductivity, E_a is the activation energy, and k_B is the Boltzmann constant. The conductivity was measured at 35K , and the activation energy calculated from the slopes of the lines is given in Table (3). It seems that the arsenic incorporation induced an improvement of the electrical conductivity (σ) with a decrease of its activation energy (E_a). These results can be related to the shift of the Fermi level towards the conduction band due to arsenic doping and also due to the of tellurium concentration; the effect of the tellurium concentration is not significant, as it was observed that as the tellurium concentration decreases in the sample composition and the arsenic-doped increases, the electrical properties improve. However, (p-type) for electrical conductivity in the sample composition is (p-type); similarly for holes. Usually shows p-type conductivity, it is difficult to grow the low conductivity n-type. This is because of the self-compensation mechanism. The films exhibited very high conductivity by increasing the dopant concentration, which leads to the carrier concentration increasing significantly. The electrical measurements under white light revealed that the presence of arsenic or tellurium in the films leads to a degradation of their light sensitivity.

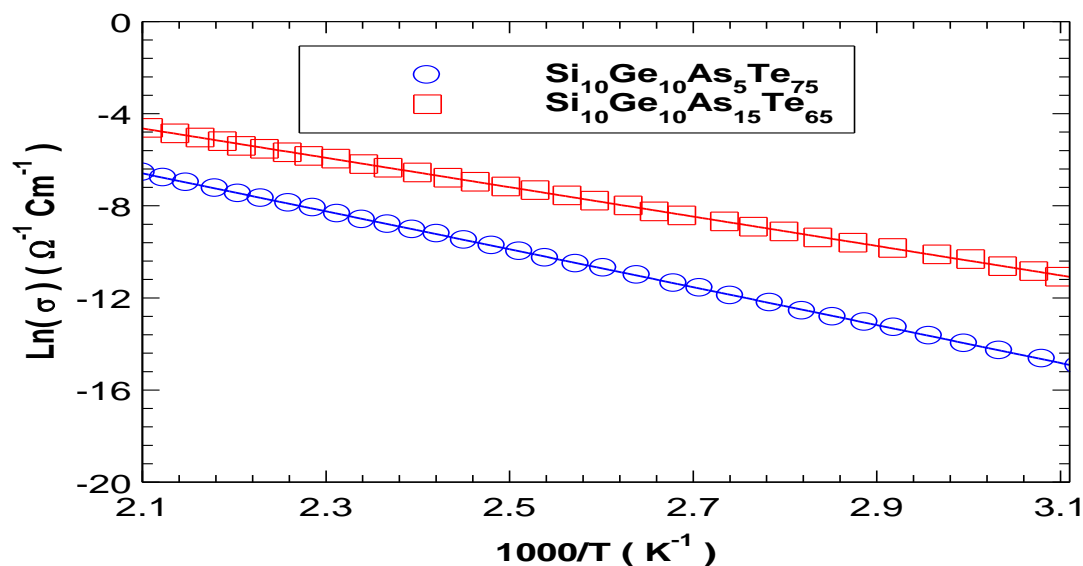


Figure (4): Logarithm of electrical conductivity vs. inverse of temperature for As-doped (dAs=15nm and 45nm) $\text{Si}_{10}\text{Ge}_{10}\text{As}_x\text{Te}_{80-x}$ system (where $x=5$ and 15).

Table (3): The data of activation energy (E_a) and electrical conductivity (σ) for samples annealed at 400°C for 2 h.

The sample	As-doped (nm)	$\sigma(\Omega^{-1}.\text{cm}^{-1})$	$E_a(\text{eV})$
Si ₁₀ Ge ₁₀ As ₅ Te ₇₅	15nm	0.21×10^{-6}	0.71
Si ₁₀ Ge ₁₀ As ₁₅ Te ₆₅	45nm	9.83×10^{-6}	0.54

ii. The influence of annealing time on electrical conductivity and kinetic constants

The conductivity as a function of the annealing time at constant temperatures for As-doping ($d_{\text{As}}=15$ nm and 45nm) of Si₁₀Ge₁₀As_xTe_{80-x} system (where $x=5$ and 15) is shown in the figures (5) and (6), respectively. The increase of electrical conductivity with increasing the annealing time at constant temperatures of 473, 573, and 673 K is due to the crystallization effects occurring only in the Ge matrix; it is clear from X-ray, and also the arsenic incorporation induced for internal surface voids and between multilayers of the sample. Doping with arsenic eliminates defects and improves electrical properties, but n-type conductivity is difficult to grow due to the self-compensation mechanism, resulting in p-type conductivity.

The electrical conductivity and the activation energy for As-doped of the system Si₁₀Ge₁₀As_xTe_{80-x} (where $x=5$ and 15) are affected by annealing temperature while the electrical conductivity increases and the activation energy decreases noticeably due to dopant segregation. The activation of arsenic atoms passivated by germanium can occur at the annealing temperature through dissociation of bridging Ge-Ge-As bonds; this behavior also appeared in another study of boron-doped hydrogenated amorphous silicon [20]. The same behavior was obtained for films annealed at constant temperatures higher than the substrate temperature, as shown in Figures (5) and (6). Thus, the electrical conductivity measurements as a function of annealing time at constant temperature are used to study the isothermal crystallization kinetics using Johnson-Mehl-Avermi's (JMA) equation in the form [21]: $\chi=1-\exp[-kt^n]$ where χ is the volume fraction of the crystalline phases transformed from the amorphous state at time t , n refers to the order of reaction, and k is the effective overall reaction rate, which actually reflects the rate of crystallization and is given by: $k=k_0\exp[-E_c/RT]$ here k_0 indicates the number of attempts to overcome the energy barrier.

The electrical conductivity as a function of annealing time, the volume fraction χ , is: $\chi=(\text{Ln}\sigma_a-\text{Ln}\sigma_t)/(\text{Ln}\sigma_a-\text{Ln}\sigma_c)$ where $\text{Ln}\sigma_a$ is the logarithm of the electrical conductivity at zero time (activation electrical conductivity), $\text{Ln}\sigma_t$ logarithm of the electrical conductivity at any time t and $\text{Ln}\sigma_c$ ithe logarithm of the electrical conductivity at the end of saturation (full crystallization). According to the JMA equation, the value of n can be obtained from the slopes of the plots of $\text{Ln}[-\text{Ln}(1-\chi)]$ vs. Lnt that are measured for this material. Since the volume fraction of the crystallized phases is assumed to be depending on the electrical conductivity of the material at any annealing time, the value of n can depend on the composition and annealing temperature in this study. The values of k according to JMA equation are obtained from the slopes of the plots of $-(1-\chi)$ vs. (t^n) . The values of the activation energies E_c of crystallization can be deduced from the slopes of the plots of $\text{Ln}k$ vs. $1000/T$ [22,23]. According to the JMA equation, the results obtained for n , k , and the activation energy E_c of crystallization for the system Si₁₀Ge₁₀As_xTe_{80-x} (where x at 5 and 15 %) measured at 473, 573, and 673K illustrated in figure (5) are also given in Table (4).

The study shows that increasing doping leads to a higher crystallization rate, resulting in a decrease in the activation energy E_c of crystallization.

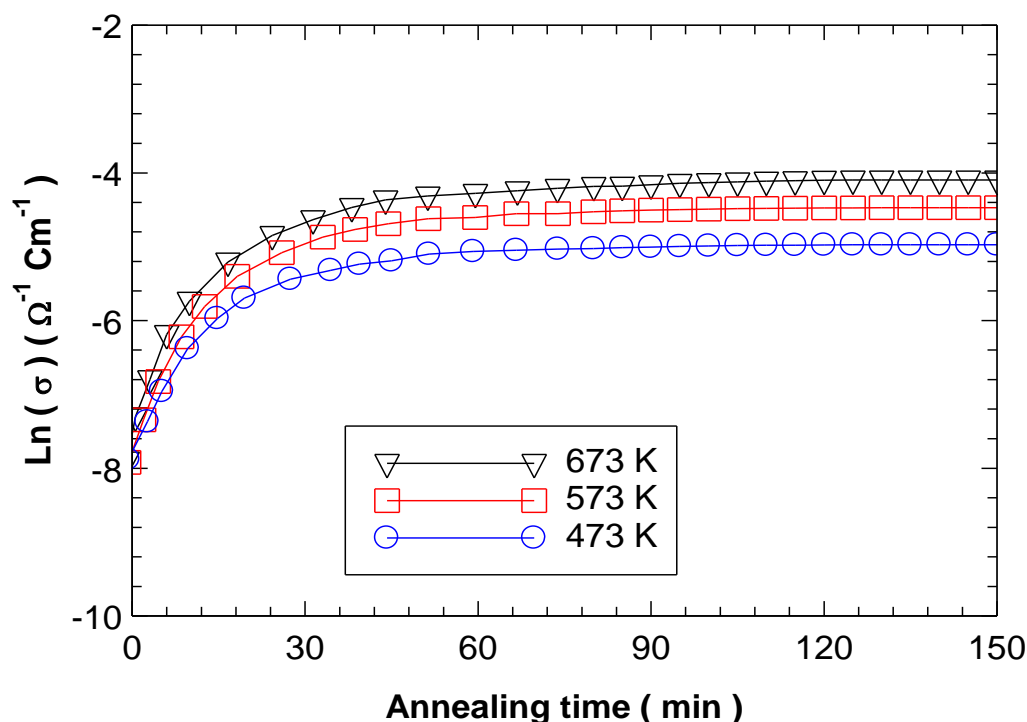


Figure (5): Logarithm of the electrical conductivity versus the annealing time at constant temperatures for As-doped of the system $\text{Si}_{10}\text{Ge}_{10}\text{As}_5\text{Te}_{75}$ where $d_{\text{As}}=15\text{nm}$.

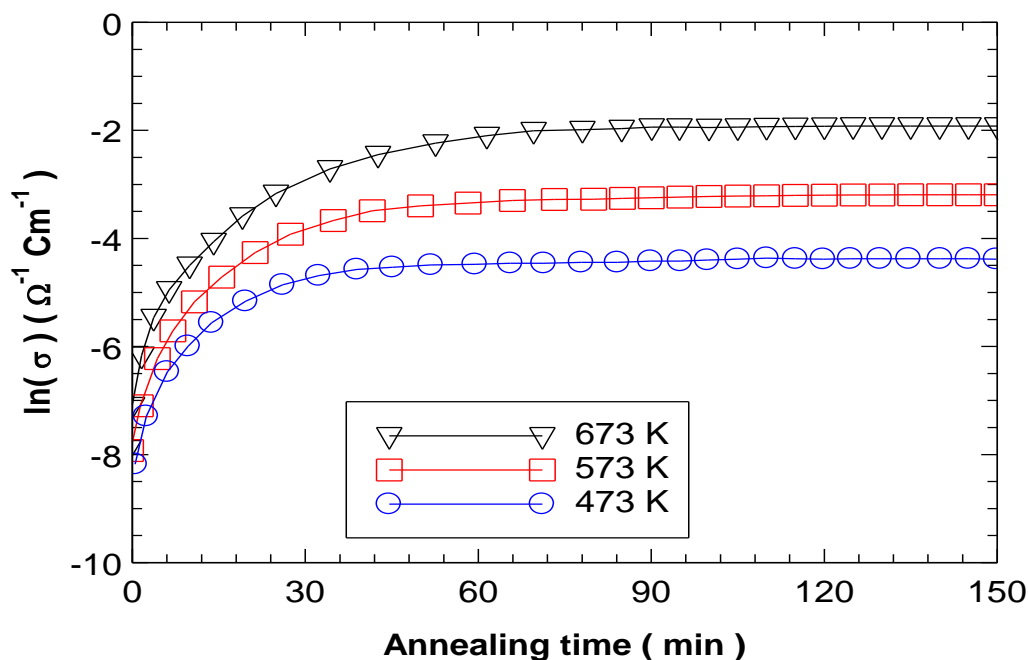


Figure (6): Logarithm of the electrical conductivity versus the annealing time at constant temperatures for As-doped of the system $\text{Si}_{10}\text{Ge}_{10}\text{As}_{15}\text{Te}_{65}$ where $d_{\text{As}}=45\text{ nm}$.

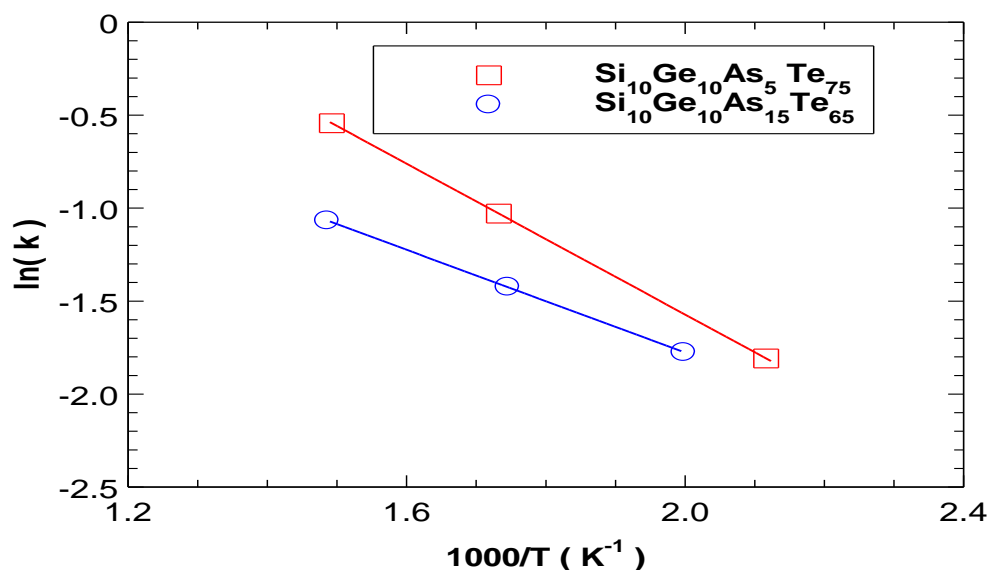


Figure (7): Plots of $\ln k$ vs. $1000/T$ for the As-doped $\text{Si}_{10}\text{Ge}_{10}\text{As}_x\text{Te}_{80-x}$ amorphous system.
 Table (4): Values of n , k , and E_c for the As-doped $\text{Si}_{10}\text{Ge}_{10}\text{As}_x\text{Te}_{80-x}$ amorphous system.

T	N			K			E_c kJ/mol
	473 (K)	573 (K)	673 (K)	473 (K)	573 (K)	673 (K)	
x=5	0.730	0.688	0.579	1.63×10^{-1}	3.59×10^{-1}	5.79×10^{-1}	16.9
x=15	0.720	0.682	0.631	1.81×10^{-1}	2.41×10^{-1}	3.44×10^{-1}	11.5

iii. Charge carrier decay lifetime measurements.

Time-resolved photoluminescence measurements were carried out to measure the recombination lifetime of the prepared sample. It is known that fast recombination isn't preferred in semiconductor devices. It is due to structural defects and trapping shallow energy levels. Here, the samples have a long lifetime. It is about 79.8 ns; see figure (8). It makes the sample promising in semiconductor industries.

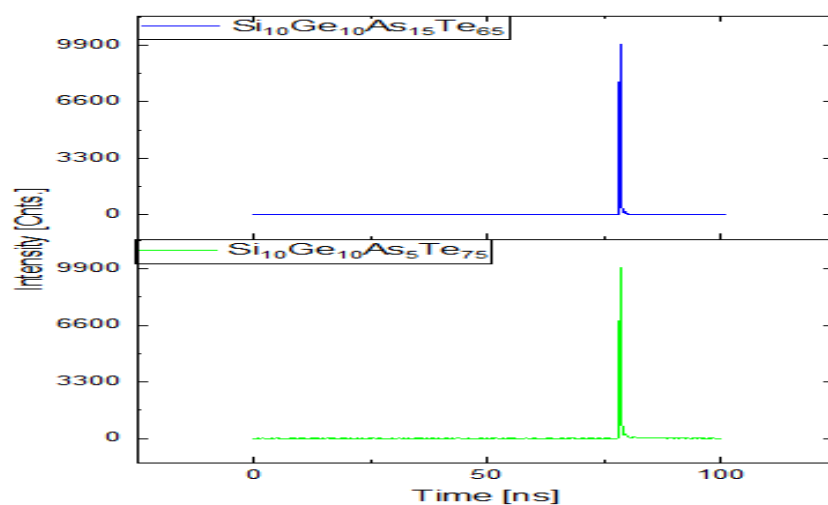


Figure (8): Time-resolved photoluminescence of the As-doped $\text{Si}_{10}\text{Ge}_{10}\text{As}_x\text{Te}_{80-x}$ amorphous system.

iv. Photoluminescence measurements

To investigate the optical transitions of a material, photoluminescence measurement is used for that. Figure (9) shows the optical transitions of the prepared samples. It is observed that the samples have one strong transition at 752 nm (1.65 eV) and another weak transition at 564 nm (2.19 eV) that obtained from UV-V is spectroscopy measurements. $\text{Si}_{10}\text{Ge}_{10}\text{As}_{15}\text{Te}_{65}$ has higher intensity of transitions due to the higher As content than $\text{Si}_{10}\text{Ge}_{10}\text{As}_5\text{Te}_{75}$.

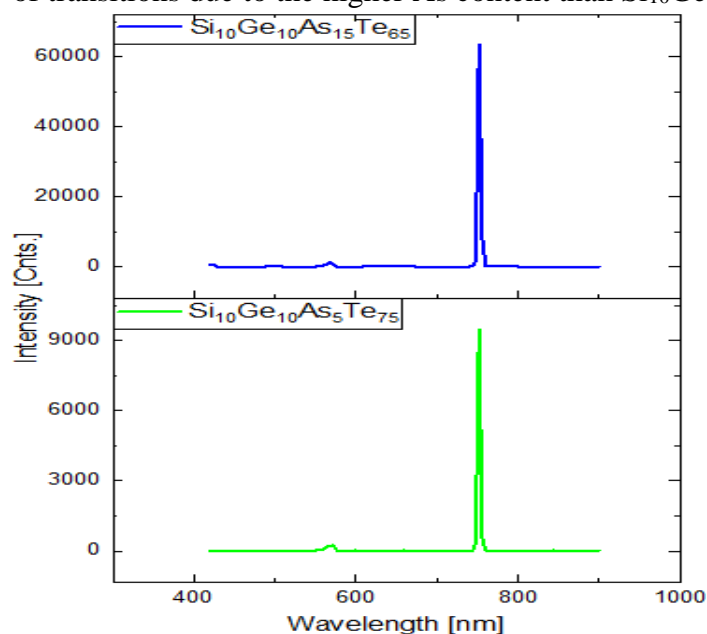


Figure (8): Photoluminescence spectra of As-doped $\text{Si}_{10}\text{Ge}_{10}\text{As}_x\text{Te}_{80-x}$ amorphous system.

IV. Conclusions

The elements such as tellurium and doped-arsenic have been added to the Si-Ge system to improve the different properties, and we have investigated the optical properties of the $\text{Si}_{10}\text{Ge}_{10}\text{As}_x\text{Te}_{80-x}$ films that show a reduction behavior in dispersion parameters with the increment in As content. It is clear that the change of the electrical conductivity with annealing time at different isotherms is one of the sensitive physical properties that reflects the change and growth of the phase transformation process of any material. The change of the electrical conductivity confirms the sensitivity of the thin film to light. The electrical conductivity and the activation energy are affected by annealing temperature, where the activation energy decreases. The optical energy gap is decreased and the Urbach energy is increased with increasing the arsenic-doped (As-doped) and raising annealing temperature and partially due to crystallization effects in the Ge matrix. The activation energy of the crystallization process (E_c) is a function of both material composition and temperature. The results revealed that (E_c) increases and the electrical conductivity increases with raising the As content. Finally the samples have a long lifetime; it is about 79.8 ns. It makes the sample promising in semiconductor industries. In photoluminescence measurements, the increasingly higher intensity of transitions is due to the increasing arsenic content.

Acknowledgements

My great thanks are due to Dr. Mohamed Nawwar, at the physics Department, Faculty of Science, Menoufia University, Egypt, for his kind and immensely helpful assistance in achieving my goals. This work is sponsored by the Libyan Ministry of Higher Education and Benghazi University.

References

- [1] Ghazala, M. S. A., Aboelhasn, E., Amar, A. H., & Gamel, W. (2011). Thermal stability and electrical properties of $\text{Se}_{90}\text{Ge}_{10-x}\text{In}_x$ amorphous alloys. *Physica Status Solidi. C, Conferences and Critical Reviews/Physica Status Solidi. C, Current Topics in Solid State Physics*, 8(11–12), 3095–3098. <https://doi.org/10.1002/pssc.201000562>.
- [2] Popescu, M., Sava, F., Velea, A., & Lőrinczi, A. (2009). Crystalline–amorphous and amorphous–amorphous transitions in phase-change materials. *Journal of Non-Crystalline Solids*, 355(37–42), 1820–1823. <https://doi.org/10.1016/j.jnoncrysol.2009.04.053>.
- [3] Ovshinsky, S. R. (1968). Reversible Electrical Switching Phenomena in Disordered Structures. *Physical Review Letters*, 21(20), 1450–1453. <https://doi.org/10.1103/physrevlett.21.1450>.
- [4] Lacaita, A. (2006). Phase change memories: State-of-the-art, challenges and perspectives. *Solid-State Electronics*, 50(1), 24–31. <https://doi.org/10.1016/j.sse.2005.10.046>.
- [5] Lok Chow, Thermoelectric Power and DC Conductivity of Amorphous $\text{Ge}_{10}\text{Si}_{12}\text{As}_{30}\text{Te}_{48}$ Semiconductors, University of Manitoba, 1976.
- [6] Garbin, D., Devulder, W., Degraeve, R., Donadio, G. L., Clima, S., Opsomer, K., Fantini, A., Cellier, D., Kim, W. G., Pakala, M., Cockburn, A., Detavernier, C., Delhougne, R., Goux, L., & Kar, G. S. (2019). Composition Optimization and Device Understanding of Si-Ge-As-Te Ovonic Threshold Switch Selector with Excellent Endurance. *2021 IEEE International Electron Devices Meeting (IEDM)*. <https://doi.org/10.1109/iedm19573.2019.8993547>.
- [7] Bhumia, S., Bhattacharya, P., & Bose, D. (1996). Pulsed laser deposition of ZnTe thin films. *Materials Letters*, 27(6), 307–311. [https://doi.org/10.1016/0167-577x\(96\)00009-2](https://doi.org/10.1016/0167-577x(96)00009-2).
- [8] Ibrahim, A. (2006). DC electrical conduction of zinc telluride thin films. *Vacuum*, 81(4), 527–530. <https://doi.org/10.1016/j.vacuum.2006.07.012>.
- [9] Nirmal, M., Dabbousi, B. O., Bawendi, M. G., Macklin, J. J., Trautman, J. K., Harris, T. D., & Brus, L. E. (1996). Fluorescence intermittency in single cadmium selenide nanocrystals. *Nature*, 383(6603), 802–804. <https://doi.org/10.1038/383802a0>.
- [10] McDonald, S. A., Konstantatos, G., Zhang, S., Cyr, P. W., Klem, E. J. D., Levina, L., & Sargent, E. H. (2005). Solution-processed PbS quantum dot infrared photodetectors and photovoltaics. *Nature Materials*, 4(2), 138–142. <https://doi.org/10.1038/nmat1299>.
- [11] Nozik, A. (2002). Quantum dot solar cells. *Physica E Low-dimensional Systems and Nanostructures*, 14(1–2), 115–120. [https://doi.org/10.1016/s1386-9477\(02\)00374-0](https://doi.org/10.1016/s1386-9477(02)00374-0).
- [12] Nakamura, Y. (2018). Nanostructure design for drastic reduction of thermal conductivity while preserving high electrical conductivity. *Science and Technology of Advanced Materials*, 19(1), 31–43. <https://doi.org/10.1080/14686996.2017.1413918>.
- [13] Das, S., Senapati, S., Alagarasan, D., Varadharajaperumal, S., Ganesan, R., & Naik, R. (2022). Enhancement of nonlinear optical parameters upon phase transition in new quaternary $\text{Ge}_{20}\text{Ag}_{10}\text{Te}_{10}\text{Se}_{60}$ films by annealing at various temperatures for optoelectronic applications. *Journal of Alloys and Compounds*, 927, 167000. <https://doi.org/10.1016/j.jallcom.2022.167000>.
- [14] Wang, B., Fu, X., Song, S., Chu, H., Gibson, D., Li, C., Shi, Y., & Wu, Z. (2018). Simulation and optimization of film thickness uniformity in physical vapor deposition. *Coatings*, 8(9), 325. <https://doi.org/10.3390/coatings8090325>.
- [15] Tauc, J. (1974). Amorphous and Liquid Semiconductors. In *Springer eBooks*. <https://doi.org/10.1007/978-1-4615-8705-7>.
- [16] Tillack, B., Zaumseil, P., Morgenstern, G., Krüger, D., Dietrich, B., & Ritter, G. (1995). Strain compensation in ternary $\text{Si}_{1-x-y}\text{Ge}_x\text{B}_y$ films. *Journal of Crystal Growth*, 157(1–4), 181–184. [https://doi.org/10.1016/0022-0248\(95\)00405-x](https://doi.org/10.1016/0022-0248(95)00405-x).

- [17] Urbach, F. (1953). The Long-Wavelength Edge of Photographic Sensitivity and of the Electronic Absorption of Solids. *Physical Review*, 92(5), 1324. <https://doi.org/10.1103/physrev.92.1324>.
- [18] Amanullah, F. M., Al-Shammari, A. S., & Al-Dhafiri, A. M. (2005). Co-activation effect of chlorine on the physical properties of CdS thin films prepared by CBD technique for photovoltaic applications. *Physica Status Solidi (A)*, 202(13), 2474–2478. <https://doi.org/10.1002/pssa.200420075>.
- [19] Abo-Ghazala, M. S. (2011). Effect of H-dilution and hydrogen bonding configuration on optical and electronic properties of a-Si:H/a-Ge:H multilayers. *Physica Status Solidi. C, Conferences and Critical Reviews/Physica Status Solidi. C, Current Topics in Solid State Physics*, 8(11–12), 3099–3102. <https://doi.org/10.1002/pssc.201000561>.
- [20] Khelifati, N., Tata, S., Rahal, A., Cherfi, R., Fedala, A., Kechouane, M., & Mohammed-Brahim, T. (2010). The annealing temperature effect on the electrical properties of boron-doped hydrogenated amorphous silicon a-Si:H(B). *Physica Status Solidi. C, Conferences and Critical Reviews/Physica Status Solidi. C, Current Topics in Solid State Physics*, 7(3–4), 679–682. <https://doi.org/10.1002/pssc.200982718>.
- [21] Augis, J. A., & Bennett, J. E. (1978). Calculation of the Avrami parameters for heterogeneous solid state reactions using a modification of the Kissinger method. *Journal of Thermal Analysis*, 13(2), 283–292. <https://doi.org/10.1007/bf01912301>.
- [22] Rao, C. N. R., & Rao, J. N. K. (1978). Phase transitions in solids : an approach to the study of the chemistry and physics of solids. In *McGraw-Hill eBooks*. <https://ci.nii.ac.jp/ncid/BA09886264>.
- [23] El-Zaidia, M.M. and Nassar, A.M., 1981. Amorphous-crystalline transformation and X-ray studies of Se₈₀Te₁₈S₂. *Physics and Chemistry of Glasses*, 22, pp.147-9.

الخصائص التركيبية والبصرية والكهربائية لنظام $\text{Si}_{10}\text{Ge}_{10}\text{As}_x\text{Te}_{80-x}$ غير المتبلور

طارق محمد فايز
قسم الفيزياء كلية العلوم، جامعة سبها، ليبيا

ابراهيم عبدالحفيظ صالح
قسم الفيزياء كلية الاداب والعلوم الابيار، جامعة بنغازي، ليبيا

الملخص

تمت دراسة الأغشية الرقيقة للنظام $\text{Si}_{10}\text{Ge}_{10}\text{As}_x\text{Te}_{80-x}$ (حيث $x=5$ and 15) المحضرة عند درجة حرارة 80 درجة مئوية في نطاقات درجات الحرارة 200 و 300 و 400 درجة مئوية. تتكون الطبقتان المتعددتان من الأغشية الرقيقة من السيليكون (Si) والجرمانيوم (Ge) والتيلوريوم (Te) المشوب بالزرنيخ (As). تم تغيير درجة حرارة التلدين لتحقيق في تأثيرها على الخصائص التركيبية والكهربائية للأغشية. تم تحليل البنية البلورية وتأثير التلدين على البنية بواسطة حيود الأشعة السينية. أوضحت بيانات الأشعة السينية للأغشية الملدنة عند درجة حرارة 400 درجة مئوية بعض اطوار التبلور Ge-Ge. تم العثور على تناقص فجوة الطاقة الضوئية للأغشية المشوبة بالزرنيخ. وقد تبين أنه مع زيادة محتوى الزرنيخ في الأغشية، تزداد موصليتها أيضاً. أظهرت القياسات البصرية أن فجوة الطاقة البصرية E_g تتناقص أو تزداد عند التلدين، ويرجع هذا التزايد جزئياً إلى تأثيرات التبلور. أما القياسات الكهربائية، فقد أجريت عند درجات حرارة تلدين وأوقات تلدين مختلفة. وأظهرت النتائج أن طاقة فجوة النطاق تتناقص من 2.49 إلى 1.22 إلكترون فولت مع زيادة محتوى الزرنيخ. علاوة على ذلك، يؤدي إضافة الزرنيخ إلى انخفاض طاقات تنشيط التبلور وزيادة الموصلية. تبلغ طاقات تنشيط التبلور في أنظمة $\text{Si}_{10}\text{Ge}_{10}\text{As}_x\text{Te}_{80-x}$ المشوبة بالزرنيخ (15 نانومتر) والزرنيخ (45 نانومتر) 16.9 و 11.5 كيلوجول/مول على التوالي.

استلمت الورقة بتاريخ
2025/06/22، وقبلت
بتاريخ 2025/07/08،
ونشرت بتاريخ
2025/07/09

الكلمات المفتاحية:

نظام متعدد الطبقات،
فجوة النطاق الضوئي،
طاقات التنشيط،
التوصيل الكهربائي،
التألق الضوئي